Theor Appl Climatol
DOI 10.1007/s00704-014-1355-0

ORIGINAL PAPER

Precipitable water vapor and its relationship with the Standardized Precipitation Index: ground-based GPS measurements and reanalysis data

Isabella Bordi · Xiuhua Zhu · Klaus Fraedrich

Received: 29 January 2014 / Accepted: 18 December 2014

Abstract Monthly means of ground-based GPS measurements of precipitable water vapor (PWV) from six stations in the USA covering the period January 2007–December 2012 are analyzed to investigate their usefulness for monitoring meteorological wet/dry spells. For this purpose, the relationship between PWV and the Standardized Precipitation Index (SPI) on 1-month timescale is investigated. The SPI time series at grid points close to the stations are computed using gridded precipitation records from the NOAA Climate Prediction Center (CPC) unified precipitation dataset (January 1948–April 2012). GPS measurements are first verified against PWV data taken from the latest ECMWF reanalysis ERA-Interim; these PWV reanalysis data, which extend back to 1979, are then used jointly with CPC precipitation to compute precipitation efficiency (PE), defined as the percentage of total water vapor content that falls onto the surface as measurable precipitation in a given time period. The overall results suggest that (i) PWV time series are dominated by the seasonal cycle with maximum values during summer months, (ii) the comparison between GPS and ERA-Interim PWV monthly data shows good agreement with differences less than 4 mm, (iii) at all stations and for almost all months, PWV is only poorly correlated with recorded precipitation and the SPI, while PE correlates highly with the SPI, providing an estimate of the water availability at a given location and useful information on wet/dry spell occurrence, and (iv) long data records would allow, for each month of the year, the identification of PE thresholds associated with different SPI classes that, in turn, have potential for forecasting meteorological wet/dry spells. Thus, it is through PE that ground-based GPS measurements appear of relevance for assessing wet/dry spells, although there is not a direct relationship between PWV and SPI.

This paper is dedicated to Alfonso Sutera (1950–2013) who firmly believed that ground-based GPS measurements have great potentials not yet fully exploited.

I. Bordi (✉)
Department of Physics, Sapienza University of Rome, Rome, Italy
e-mail: isabella.bordi@roma1.infn.it

X. Zhu
Universität Hamburg, Klima Campus, Hamburg, Germany
e-mail: xiuhua.zhu@zmaw.de

K. Fraedrich
Max Planck Institute für Meteorologie, Hamburg, Germany
e-mail: klaus.fraedrich@zmaw.de

1 Introduction

Water vapor is the most abundant atmospheric greenhouse gas without which the planet's surface temperature would be well below freezing (a relatively simple treatment of traditional greenhouse ideas is given in Houghton (1977)). Phase changes involving water vapor (i.e., condensation and evaporation processes) are associated with exchanges of latent heat energy that affect the vertical stability of the atmosphere, the structure and evolution of storm systems, and the energy balance of the global climate system. Water vapor is also the main source of atmospheric hydroxyl radical, an oxidizing agent that cleanses the atmosphere of many air pollutants. Thus, it plays an important role in many processes acting in the atmosphere over a wide range of spatial and temporal scales.

Precipitable water vapor (PWV) is a measure of the total water vapor contained in a vertical air column above a site and is expressed as the resulting height of liquid water if all vapour in the column was condensed. Although the total water vapor in the atmosphere could never be released, the amount of PWV, along with the rates of inflow, gives an indication of the maximum potential precipitation and the supply of latent

Published online: 04 January 2015

heat available to develop and maintain storm processes. On the other hand, the quantity of precipitation received by a station is not only controlled by the amount of available water vapor in the air (PWV) but also controlled by the initial degree of saturation of water vapor and the dynamic mechanisms that provide the cooling necessary to produce saturation, cause the water vapor to condense, and form droplets large enough to fall to the Earth's surface. For this reason, in most cases, the actual amount of precipitation is found to be more closely related to the dynamic mechanisms of convergence and uplift than to PWV.

A measure of the effectiveness of dynamic mechanisms in releasing air moisture is the precipitation efficiency (PE), which was originally defined as the percentage of the average PWV that falls to the surface as measurable precipitation per day (Tuller 1971; Lutz 1977). More recently, other definitions have been proposed that are mainly based on condensation rate (a cloud microphysical view) or moisture flux in the convective systems (a large-scale view) (Sui et al. 2007).

Nevertheless, and despite the importance, knowledge of PWV is limited owing to the lack of high-spatiotemporal-resolution observations. Bevis et al. (1992) introduced a new approach (compared to radiosondes or space-based remote soundings at infrared and microwave wavelengths) for remote sensing of PWV that is based on ground-based GPS. The technique can provide PWV data with high temporal resolution (<1 h) in all weather conditions and during both daytime and nighttime. It relies on the measurements of the atmospheric delay radio signals (L band at frequencies of 1.22760 and 1.57542 GHz) that are transmitted from GPS satellites through the ionosphere and the electrically neutral atmosphere.

Since the ionospheric delay is dispersive, it can be removed from the two carrier frequencies of GPS satellites (Brunner and Gu 1991; Zhang et al. 1999). The remaining delay, which is referred to as the tropospheric delay, is determined by the refractive index along the slant signal path depending on the azimuth and elevation of each satellite. Thus, the zenith tropospheric delay (ZTD) at a GPS site is estimated by mapping slant delays to zenith-equivalent values with a zenith-angle-dependent mapping function, usually assumed to be azimuthally symmetric.

The refractivity of the atmosphere is a function of temperature, pressure, and water vapor content, and water vapor is the only gas in the troposphere that has a permanent dipole moment that contributes to the dipolar component of the atmospheric refractivity. Thus, ZTD can be conveniently divided into a hydrostatic delay (ZHD), associated with the dipole moment induced by the dry atmosphere, and into a wet delay (ZWD), associated with the permanent dipole moment of water vapor (Saastamoinen 1972).

The ZTD can be calculated from actual measurements at GPS receivers using complex inversion algorithms (e.g., Duan et al. 1996). The ZHD can be modeled using surface pressure data, while ZWD is obtained by subtracting the ZHD from the ZTD. Subsequently, the ZWD can be transformed into PWV from the water-vapor-weighted mean temperature (Davis et al. 1985; Bordi et al. 2014b). Approximately 1 mm of PWV produces a 6.35-mm delay, but this factor can oscillate about 20 %, depending on the location, the altitude, the season, and local meteorological conditions (Bevis et al. 1994). Moreover, uncertainties induced by temperature variations depend on the absolute amount of PWV (an uncertainty of 5 K corresponds to about 1.7–2.0 % in PWV), while a variation of 1 hPa in the surface pressure corresponds to about 0.33–0.37 mm in PWV (Hagemann et al. 2003).

In the last years, the assimilation of GPS PWV into mesoscale numerical prediction models and problems related with hurricanes or floods have been widely investigated (e.g., Guerova et al. 2004; Vedel et al. 2004; Nakamura et al. 2004; Smith et al. 2007; Seco et al. 2009). Additional applications are concerned with the validation of PWV reanalysis products with GPS observations (Vey et al. 2010) or the analysis of long-term memory effects in the time series (Bordi et al. 2014a). However, only a few efforts have been devoted to investigating the possible use of ground-based GPS for monitoring drought or wet events. Some studies found that the seasonally adjusted time series of the vertical displacement of the Earth's surface measured by GPS can be used for monitoring drought-induced uplift or changes of the terrestrial water loading (Bevis et al. 2005; Borsa et al. 2014). In a recent study by Bordi et al. (2014b), the potentials of ground-based GPS measurements of PWV for hydrological applications, including the analysis of meteorological dry/wet spells, have been investigated. The authors, through a sample analysis at two GPS sites in the USA (Billings in Montana and Hartsville in Tennessee) for the time period 2009–2012, indicated that there is a general agreement between PE time series and the Standardized Precipitation Index (SPI) (as an index of drought and wetness) on 1-month timescale (their Fig. 8). The SPI, originally introduced by McKee et al. (1993), is commonly applied to assess drought and wet phenomena; the index is based only on long precipitation records, and the monthly timescale is considered suitable for characterizing meteorological wet/dry spells (Bordi and Sutera 2004; Hayes et al. 2011). Thus, it is envisaged that GPS PWV may be used to assess dry and wet spells through the computation of PE, but further analyses are necessary to corroborate those preliminary results.

The present study wishes to extend that analysis using PWV observations taken from six sample ground-based GPS stations in the USA covering the period 2007–2012. The aim is to investigate, for additional stations characterized by different climate mean conditions and longer data records, the relationship between PWV and PE and the SPI on 1-month timescale. The SPI time series at grid points close to the stations are computed using gridded precipitation records

from the NOAA Climate Prediction Center (CPC) unified precipitation dataset. The availability of GPS PWV measurements jointly with precipitation observations at grid points close to the stations allows the computation of PE following the definition by Tuller (1971). Moreover, GPS measurements are compared with PWV data taken from the latest European Centre for Medium-Range Weather Forecasts (ECMWF) reanalysis product ERA-Interim that does not assimilate ground-based GPS observations and extends back to 1979 (Dee et al. 2011).

The paper is structured as follows: Data and methods are described in Sect. 2, while the main results are presented in Sect. 3. A summary and conclusions are provided in the final section.

2 Data and methods

2.1 Data

The study is based on near-real-time ground-based GPS measurements of PWV from the SuomiNet network managed by the University Corporation for Atmospheric Research (UCAR) in Boulder, CO, USA (Ware et al. 2000). PWV data are available every 30 min and cover different time periods depending on the stations. For the present analysis, six sample GPS stations in the USA have been considered (see Table 1 for station characteristics and Fig. 1 for their locations). They are characterized by different precipitation regimes and have rather continuous records of PWV measurements with limited missing values for the common time section January 2007–December 2012.

Cosmic's Ground-Based GPS Research Group (http://www.cosmic.ucar.edu/groundbased.html) analyzes GPS data from the SuomiNet network. Real-time GPS data are retrieved hourly, and the Bernese software (Beutler et al. 1996) is used to estimate PWV. The software for real-time processing is operated by the Bernese Processing Engine (BPE) developed jointly by the University of Bern and the UCAR GPS Research Group. Processing is done with ultrarapid predicted GPS orbits estimated from the International GPS Service (IGS) global network data collected during the previous day (Rocken et al. 1997). The signal delay due to the dry atmosphere is removed using surface barometric pressure measurements and a mapping function (Niell 1996). Vertical ZWD is estimated every 30 min for each station in the network under the assumption that the delay is azimuthally isotropic and changes approximately with the cosecant of the satellite elevation angle. The dimensionless proportionality constant relating ZWD to PWV is estimated using the weighted mean temperature of the atmosphere (T_m) computed from the vertical profiles of temperature and water vapor partial pressure provided by the NCEP's Global Forecast System (GFS) model (http://www.emc.ncep.noaa.gov).

Monthly averages of daily accumulated precipitation at grid points close to GPS stations (Table 1) have been obtained from the NOAA CPC unified precipitation dataset covering the period January 1948–April 2012. The dataset is based on observations over continental USA and is derived from three sources: NOAA's National Climate Data Center (NCDC) daily Cooperative Observer Program (COOP) stations, CPC dataset (River Forecast Centers data), and daily accumulations from hourly precipitation dataset (Higgins et al. 1996, 2000). The data have been quality-controlled to eliminate duplicates and overlapping stations, and standard deviation and buddy checks were applied. Then, they have been gridded into a 0.25×0.25 mesh (140 W–60 W, 20 N–60 N) using an optimal interpolation technique (Xie et al. 2007). Figure 1 shows the good co-location of the selected GPS stations and the nearest CPC grid points.

Aiming to compare PWV measurements from GPS with the latest reanalysis product, monthly mean of daily mean PWV data of ERA-Interim (hereafter ERAI; Dee et al. 2011), covering the time section January 1979–December 2012, is considered. Data with spatial resolution of 0.25×0.25 in longitude and latitude have been retrieved from the ECMWF archive, and grid points closest to GPS stations have been taken into account (Table 1).

Table 1 Characteristics of ground-based GPS stations and CPC and ERAI grid points close to the stations

GPS stations					CPC grid points		ERAI grid points		
Station name	City, state	Latitude (°N)	Longitude (°W)	Elevation (m, above ellipsoid)	Latitude (°N)	Longitude (°W)	Latitude (°N)	Longitude (°W)	Geometric height (m)
COSA	Scottsdale, Arizona	33.569	111.882	420.38	33.625	111.625	33.50	111.75	867.83
SA11	Laramie, Wyoming	41.320	105.668	2221.72	41.125	105.625	41.25	105.50	3344.20
SG00	Grand Forks, North Dakota	47.922	97.087	278.31	47.875	97.125	47.75	97.25	345.92
SG04	Norman, Oklahoma	37.132	97.266	388.45	37.125	97.125	37.25	97.25	398.64
VALY	Lynchburg, Virginia	37.376	79.127	287.33	37.375	79.125	37.50	79.25	388.03
TXTY	Tyler, Texas	32.250	95.394	146.85	32.125	95.125	32.25	95.50	124.16

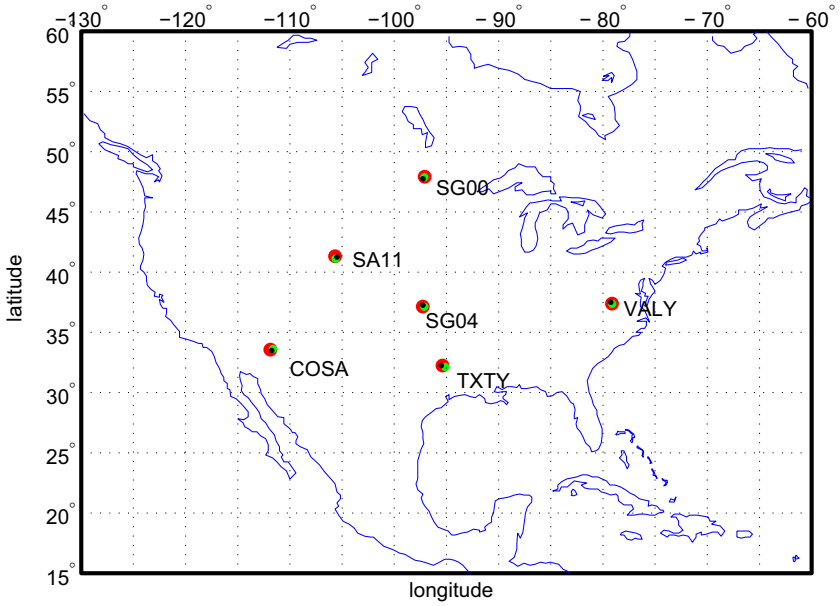

Fig. 1 Geographical location of ground-based GPS stations (*red bullets*) and nearest CPC (*green*) and ERAI grid points (*black*)

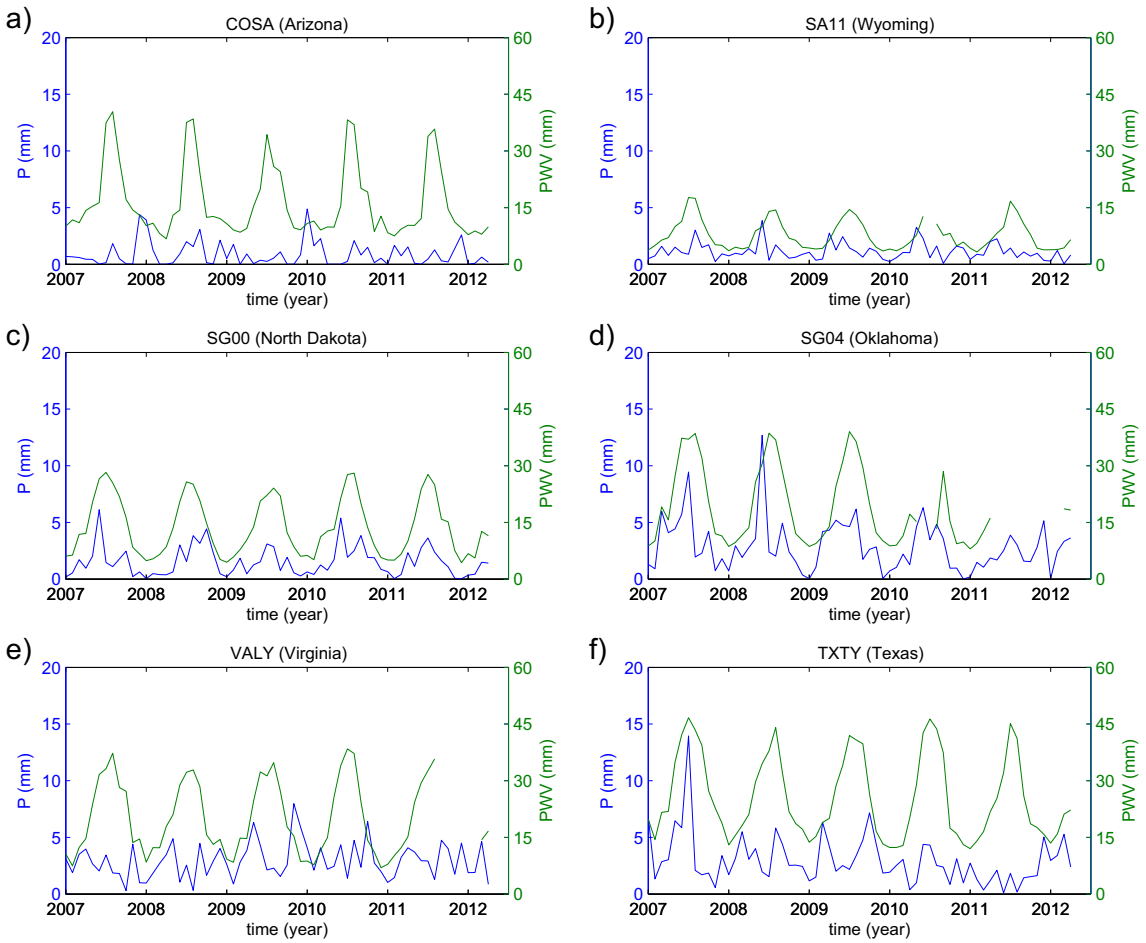

Fig. 2 Time behavior of monthly PWV at GPS stations and monthly average of daily accumulated precipitation (*P*) at nearest grid points (CPC dataset) from January 2007 to April 2012. Interruptions in PWV time series denote missing values. Units are millimeters for both PWV and P

2.2 PE and SPI

A valuable approach to assess water availability in a region is based on PE. For the purpose of the present study, we use the pioneering PE definition given by Tuller (1971), i.e., the percentage of the average PWV above a station that is released and falls to the Earth as measurable precipitation (P) in a given time period:

$$PE = \left(\frac{P}{PWV}\right)\cdot 100 \quad (1)$$

We will estimate monthly time series of PE at the six selected locations using PWV (monthly mean values) given by GPS measurements and P (monthly mean of daily accumulated precipitation) by a CPC unified precipitation dataset for the common period January 2007–April 2012. A further temporal extension (January 1979–December 2012) is provided by ERA-Interim reanalysis PWV product and by P from the CPC unified precipitation dataset, both referred to the grid points nearest to the GPS stations.

Moreover, we will investigate the possible relationship between PWV (PE) and meteorological wet/dry spells assessed by the Standardized Precipitation Index (McKee et al. 1993) computed on 1-month time scale. Details on the SPI computation can be found, for example, in Bordi and Sutera (2004) and references therein. For the purposes of the present paper, we only mention the basic concepts behind the index computation: For a given location and month of the year, long-term time series of precipitation accumulations over a given timescale are used to estimate the appropriate probability density function fitting the empirical distribution. Usually, the two-parameter gamma function or Pearson type III are used (McKee et al. 1993; Guttman 1999). The cumulative probability distribution is then transformed into a normal distribution, so that the SPI represents the number of standard deviations that the observed cumulative precipitation deviates from the climatological mean. The index can be estimated for different timescales ranging from 1 month to 2 years or more; 1-month SPI is a short-term value mostly related to meteorological drought and wetness conditions which, during the growing season, can be important for

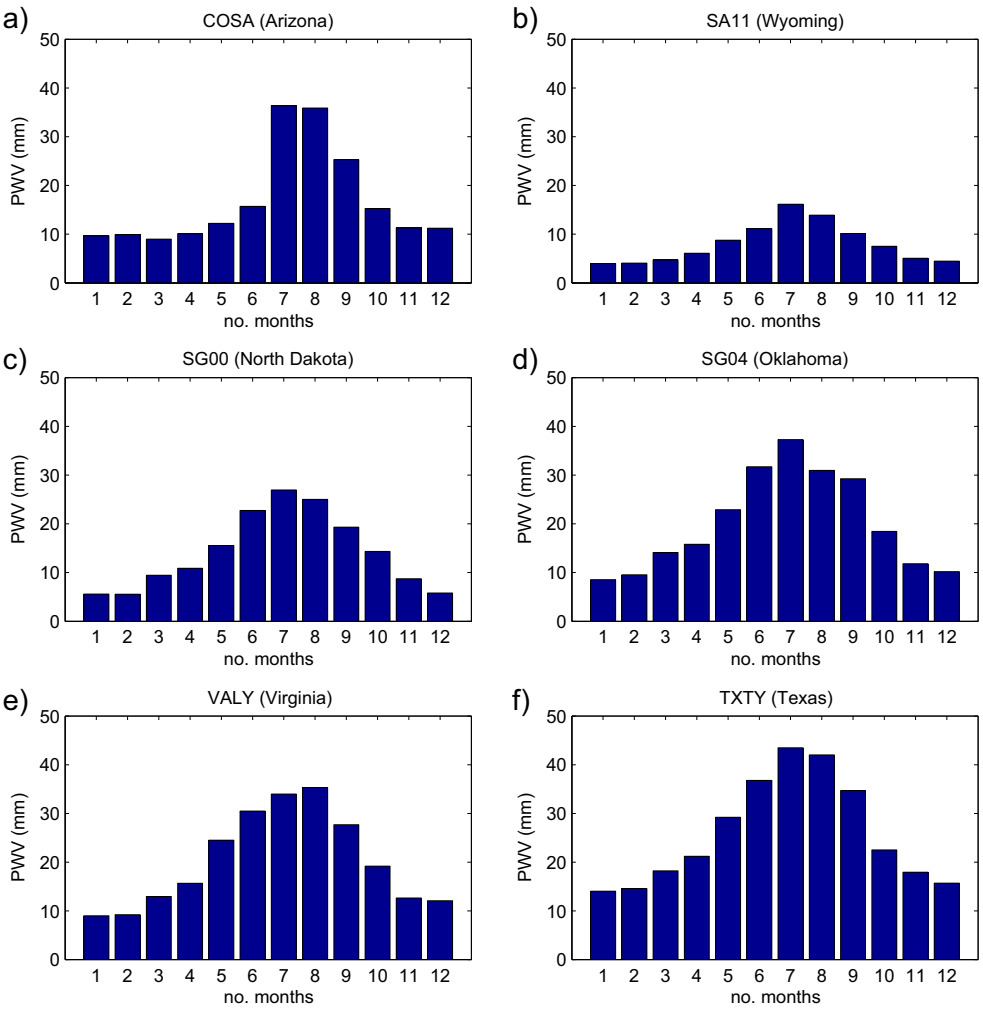

Fig. 3 Variability of PWV within the year (mean values over the period January 2007–December 2012) as measured by the six GPS stations. Units are millimeters

correlation with soil moisture and crop stress. Recently, the index was recommended by the World Meteorological Organization (WMO press release No. 872, December 2009) and by the "Lincoln declaration on drought indices" (Hayes et al. 2011) to all meteorological and hydrological services for characterizing meteorological drought. The classification of SPI values is as follows: Values between −0.99 and +0.99 denote near normal conditions, between −1 and −1.49 moderately dry, between −1.5 and −1.99 severely dry, and less than −2 extremely dry conditions. The same applies to positive values for wet classes.

3 Results

PWV measurements from six ground-based GPS stations in the USA (Fig. 1) are analyzed to investigate their relationship with local precipitation and PE. Moreover, a comparison with ERA-Interim is provided to verify the effectiveness of the reanalysis product in reproducing the monthly variability of PWV at the stations. Finally, the relationship between the SPI on 1-month time scale and PE is illustrated.

3.1 Time behavior and seasonal cycle of PWV, P, and PE

Figure 2 illustrates the time behavior (on monthly basis from January 2007 to December 2012) of GPS PWV and CPC-accumulated P at grid points nearest to the relevant stations. The figure shows that the lowest PWV values are registered at SA11 station (Wyoming), consistently with the high elevation of the GPS site (Table 1). The PWV signals exhibit a similar temporal behavior at all stations with clear minima during the winter (December–February) and maxima in the summer (June–August) following the annual temperature cycle. This

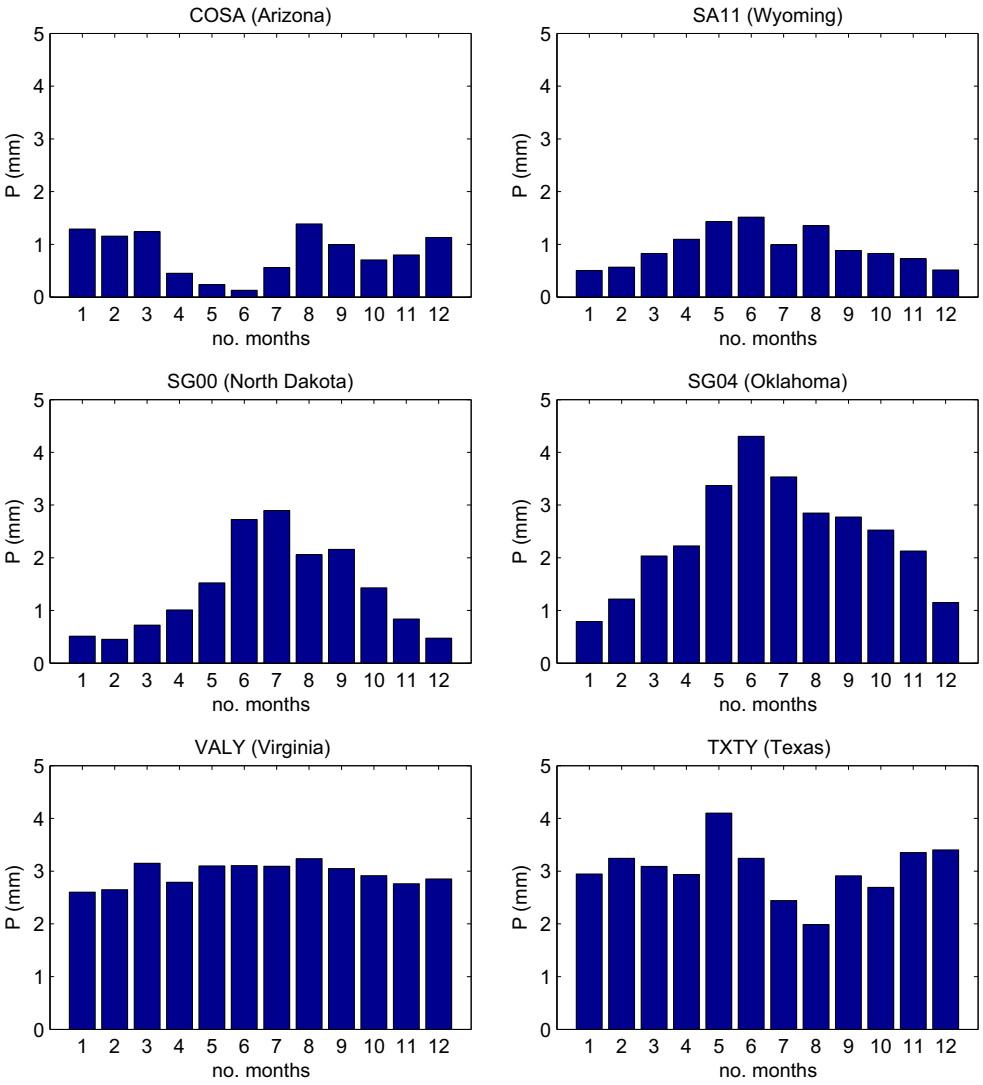

Fig. 4 Variability of monthly average of daily accumulated precipitation within the year (climatological mean conditions over the period January 1948–April 2012) at the GPC grid points close to the GPS stations. Units are millimeters

is in agreement with the humidity regimes defined by Gaffen et al. (1992). In particular, these authors found that in middle and high latitudes, PWV follows temperature, while in the tropics, the annual cycle of PWV is more closely related to midtropospheric relative humidity variations, reaching maximum values during the local rainy season when deep convection is strong (see also Bock et al. 2007; Ortis de Galisteo et al. 2013). The PWV annual cycle emerged from the spectral analysis of GPS measurements at sample SuomiNet stations in the USA (Bordi et al. 2014a).

In Fig. 2, episodes of above-normal precipitation are noticeable, such as the one that occurred during July 2007 at Tyler in Texas, i.e., about 14 mm compared to the July average of 2.4 mm (Fig. 2f). Other precipitation peaks are observed at Lynchburg in Virginia on October 2009 (Fig. 2e) or Norman in Oklahoma on July 2007 and June 2008 (Fig. 2d).

Moreover, it can be noted that usually high PWV values do not occur during the rainy months, as illustrated by the seasonal cycle of PWV and P in Figs. 3 and 4, respectively. Exceptions are SG00 (North Dakota) and SG04 (Oklahoma), which are characterized by maximum precipitation during June–July (Fig. 4c, d).

The seasonal cycle of PE, computed according to Eq. (1) using PWV from GPS measurements and P from CPC dataset for the common period January 2007–April 2012, reflects the differences observed in the seasonal variability of P and PWV between the six stations (Fig. 5). In particular, low PE values are obtained for summer months and high values for winter months at VALY and TXTY stations. However, results should be checked against longer records; an attempt to do so is given in the next subsection replacing GPS PWV measurements with ERA-Interim data (total column water vapor) extending back in time to January 1979.

3.2 GPS PWV observations and reanalysis

Assessing the effectiveness of ERA-Interim product to properly represent the monthly variability of PWV at the sample stations, we compare the GPS observations with the total column water vapor given by the reanalysis at the nearest grid

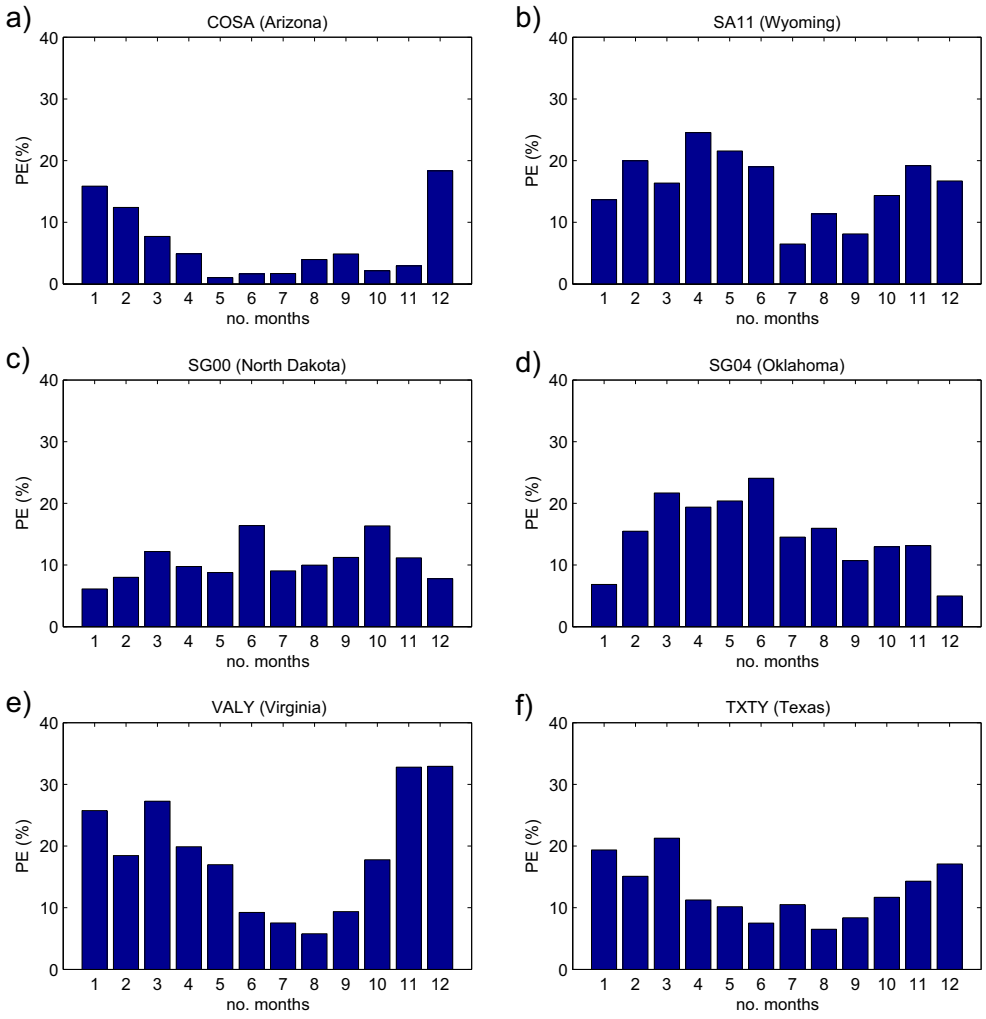

Fig. 5 Variability of PE within the year (mean values over the period January 2007–April 2012) computed using PWV from GPS measurements and P from the CPC dataset. Units are percent

points. Figure 6 illustrates the time behavior of PWV at the six selected locations for the common period January 2007–December 2012. Some differences between observations and reanalysis are found, which are particularly evident at the COSA station in Arizona (i.e., PWV values registered by GPS station appear systematically higher than the reanalysis ones). Such discrepancies, which are larger during summer months but not exceeding 7 mm and lower in the winter around 1–2 mm, are likely due to the difference in elevation: 420.38 m for the GPS station against 867.83 m of ERAI grid point (see Table 1; the geometric heights at ERAI grid points have been computed from the geopotential field taking into account the latitude dependence of gravity acceleration and of the Earth's radius). Similar considerations hold for VALY in Virginia with a difference in elevation between ERAI grid point and GPS of 100.7 m and PWV differences in the summer around 3–5 mm. Less noticeable differences are found at the other sites which are bounded between −4 and +4 mm; possibly also in these cases, the differences are related to the different elevations and not perfect co-location of ERAI grids. It is worth noticing the small differences in PWV at SA11 (Fig. 6b) although there is a large elevation difference between the GPS site and ERAI grid point; this may be explained by the scale height of water vapor in the atmosphere, which is estimated to be between 1.5 and 2 km (e.g., Ulich 1980), hence less than the elevation of the GPS site.

The availability of ERAI PWV data and CPC precipitation made it possible to compute PE for the longer time section January 1979–April 2012. The time variability of PE within the year is displayed in Fig. 7 for the six considered locations. A visual comparison with Fig. 5 suggests that the seasonal behavior previously obtained for the period January 2007–April 2012 using PWV observations is almost preserved (with smoothed month-to-month variations) when the longer period is considered.

3.3 Relationship between PWV, PE and SPI

To find a possible relationship between the integrated total column water vapor in the atmosphere and the occurrence of meteorological wet/dry events, we have investigated the correlations between P and PWV, the SPI and PWV, and the SPI and PE for each month of the year using ERAI data and CPC precipitation.

Results are reported in Table 2, where statistically significant correlation coefficients at 99 % confidence level are denoted in bold. As expected, there is a general low

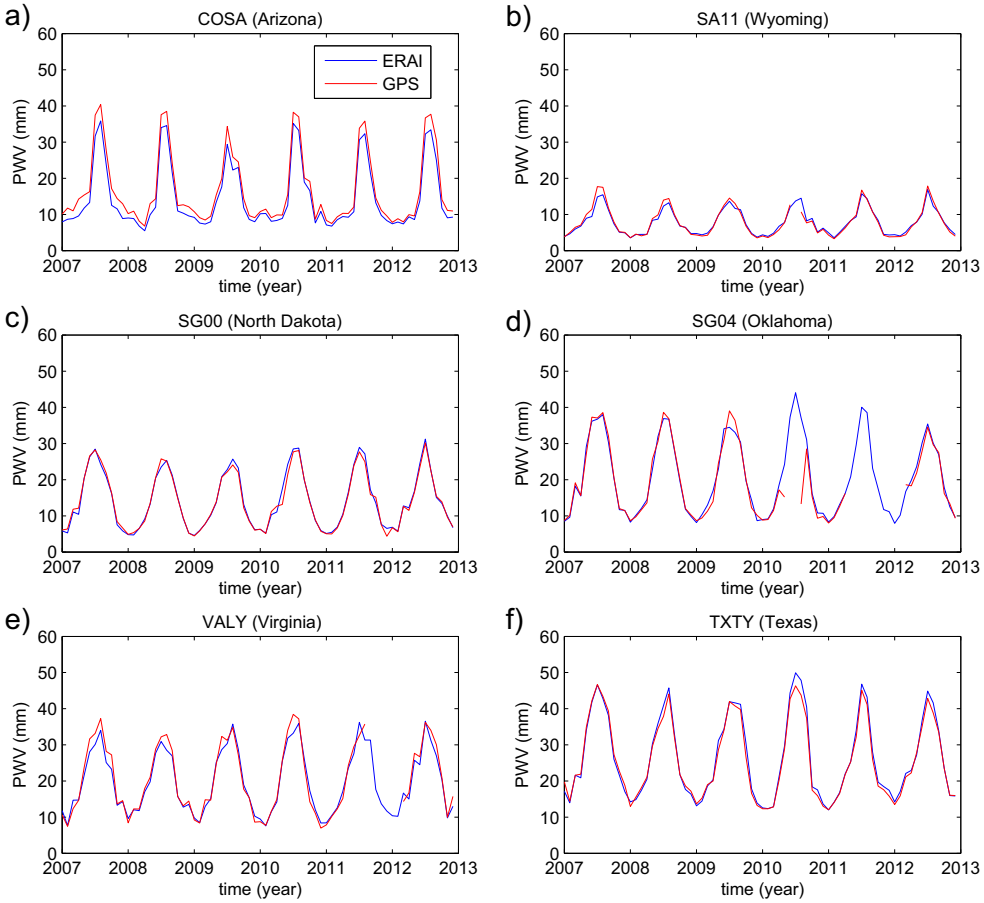

Fig. 6 Comparison between monthly PWV measured by ground-based GPS stations (*red line*) and that by ERAI reanalysis (*blue line*) from January 2007 to December 2012. Units are millimeters

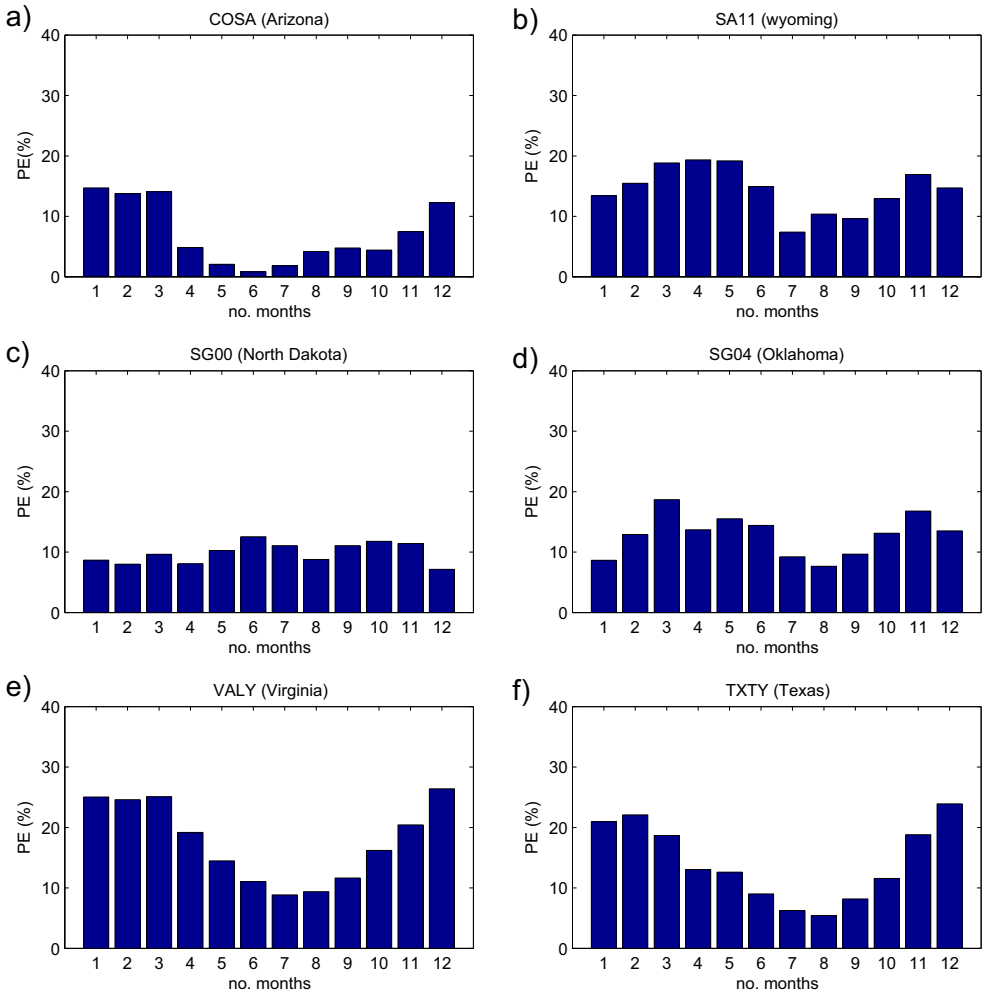

Fig. 7 Variability of PE within the year (mean values over the period January 1979–April 2012) computed using PWV from ERAI reanalysis and P from the CPC dataset. Units are percent

correlation between precipitation and PWV since precipitation received by a station (or in a given location) is controlled not only by the amount of the available water vapor in the air but also by other factors like the degree of saturation of the water vapor and the presence of dynamic mechanisms, which provide the cooling necessary to produce saturation and hence cause the water vapor to condense forming precipitation. The same applies to the correlations between the SPI and PWV since the index is based on the amount of precipitation accumulated on the monthly timescale. Instead, high correlation values are found between the SPI and PE for all months of the year and at all stations/locations. This is clearly evident in the time series of the SPI and PE from January 2007 to April 2012 at the stations (Fig. 8). High values of PE, which depend on the month of the year, are associated with wet spells (SPI greater than +1), and vice versa for dry spells (SPI less than −1).

These findings suggest that for each month of the year, PE thresholds exist, above which meteorological wet/dry spells occur with different intensity. An attempt to investigate this aspect is displayed in Fig. 9 showing scatter plots of PE versus SPI for sample months of the four seasons (i.e., January, April, July, and October). It can be noted that locations characterized by a clear seasonality of PE (see Fig. 7), such as COSA, VALY, TXTY, or SA11, show a different behavior as a function of the SPI during January, July, and the transition months April and October. In these cases, it is possible to identify PE thresholds associated to the different SPI wet classes. For example, at the COSA station, SPI values between 1.5 and 1.99 (severely wet conditions) are associated with PE around 8 % in July, about 19 % in October and April, and about 45 % in January. Thus, at a given location, the availability of long P and PWV records allows, for each month of the year, the computation of the climatological PE thresholds associated with the SPI classes. These, in turn, could be used as reference for forecasting the occurrence of future wet events.

As can be noted from the scatter plots, PE is less sensitive to the SPI for dry conditions (SPI less than −1), thus preventing the identification of distinguished PE thresholds for the various months of the year and SPI dry classes. The latter problem also occurs for locations characterized by almost uniform PE values during the year, like the station

Table 2 Correlation coefficients between P and PWV, SPI and PWV, and SPI and PE for each month of the year

Correlation	Station	Jan	Feb	Mar	Apr	May	Jun	Jul	Aug	Sep	Oct	Nov	Dec
(P, PWV)	COSA	**0.59**	**0.60**	**0.71**	0.25	**0.45**	0.02	**0.55**	0.35	−0.08	**0.51**	0.13	**0.51**
	SA11	0.11	0.17	0.36	0.03	0.09	0.20	**0.51**	0.42	0.36	0.21	0.05	0.19
	SG00	−0.20	0.36	**0.57**	0.32	0.41	0.22	0.33	0.01	0.08	**0.73**	0.05	−0.29
	SG04	**0.62**	**0.51**	**0.61**	0.17	0.11	−0.03	0.16	−0.15	−0.22	0.42	0.29	**0.55**
	VALY	**0.68**	**0.47**	0.40	−0.03	0.06	0.23	0.25	−0.09	0.31	0.10	0.38	0.07
	TXTY	**0.48**	**0.45**	0.29	0.09	0.28	**0.44**	0.38	0.01	0.32	**0.54**	0.11	0.41
(SPI, PWV)	COSA	**0.62**	**0.66**	**0.71**	0.41	**0.51**	0.28	**0.62**	0.37	0.02	0.40	0.26	**0.45**
	SA11	0.10	0.18	0.28	0.06	0.11	0.28	**0.52**	0.37	0.37	0.16	0.06	0.13
	SG00	−0.12	0.29	**0.48**	0.43	0.39	0.14	0.29	−0.02	0.12	**0.74**	−0.01	−0.26
	SG04	**0.47**	**0.50**	**0.58**	0.36	0.05	0.00	0.23	−0.13	−0.16	**0.46**	0.25	0.38
	VALY	**0.71**	**0.50**	0.38	−0.02	0.07	0.23	0.25	−0.06	0.34	0.11	0.28	0.09
	TXTY	**0.53**	**0.45**	0.34	0.03	0.29	**0.51**	0.44	0.10	0.34	**0.56**	−0.01	0.43
(SPI, PE)	COSA	**0.80**	**0.76**	**0.80**	**0.78**	**0.76**	**0.73**	**0.82**	**0.93**	**0.89**	**0.80**	**0.75**	**0.76**
	SA11	**0.95**	**0.95**	**0.94**	**0.95**	**0.97**	**0.93**	**0.97**	**0.96**	**0.94**	**0.97**	**0.93**	**0.96**
	SG00	**0.86**	**0.92**	**0.93**	**0.74**	**0.91**	**0.98**	**0.95**	**0.97**	**0.95**	**0.95**	**0.91**	**0.91**
	SG04	**0.84**	**0.81**	**0.95**	**0.78**	**0.97**	**0.97**	**0.95**	**0.97**	**0.93**	**0.93**	**0.95**	**0.81**
	VALY	**0.96**	**0.94**	**0.93**	**0.96**	**0.94**	**0.97**	**0.98**	**0.95**	**0.96**	**0.94**	**0.88**	**0.92**
	TXTY	**0.95**	**0.92**	**0.92**	**0.93**	**0.97**	**0.93**	**0.94**	**0.94**	**0.96**	**0.94**	**0.93**	**0.92**

Statistically significant coefficients at 99 % confidence level are in bold

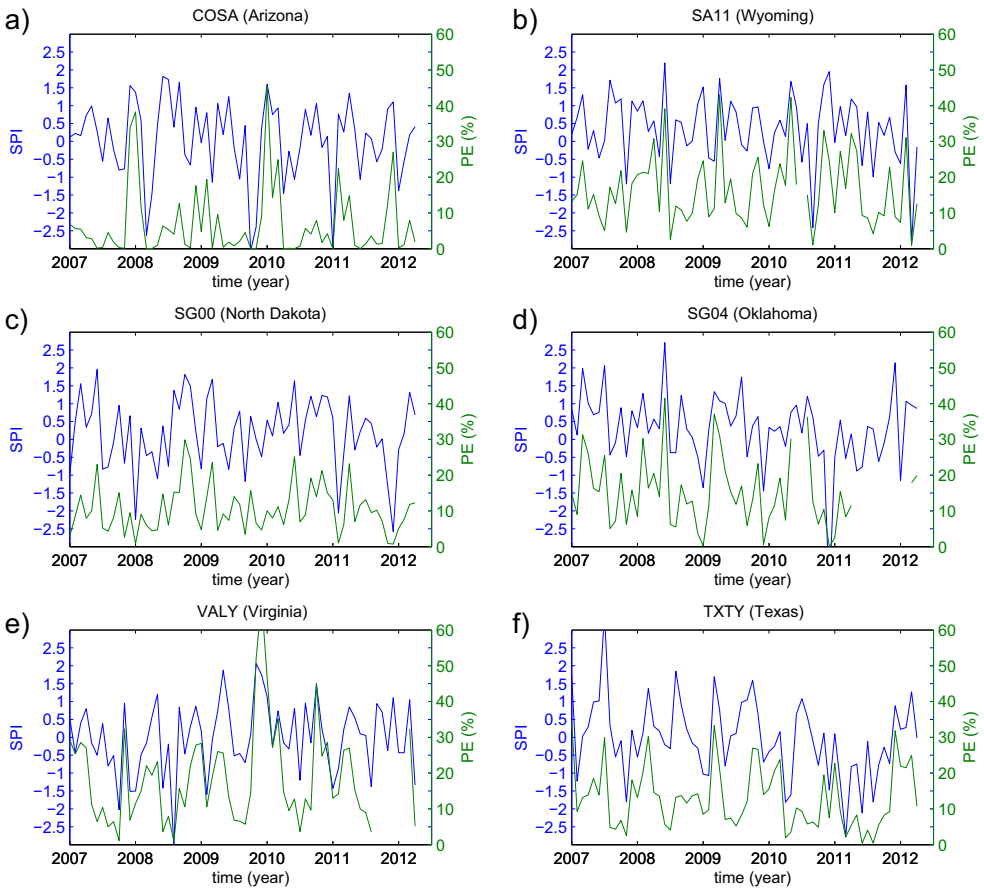

Fig. 8 Time behavior of the SPI computed using CPC precipitation data and PE computed using CPC precipitation data and PWV GPS measurements from January 2007 to April 2012. Units for PE are percent

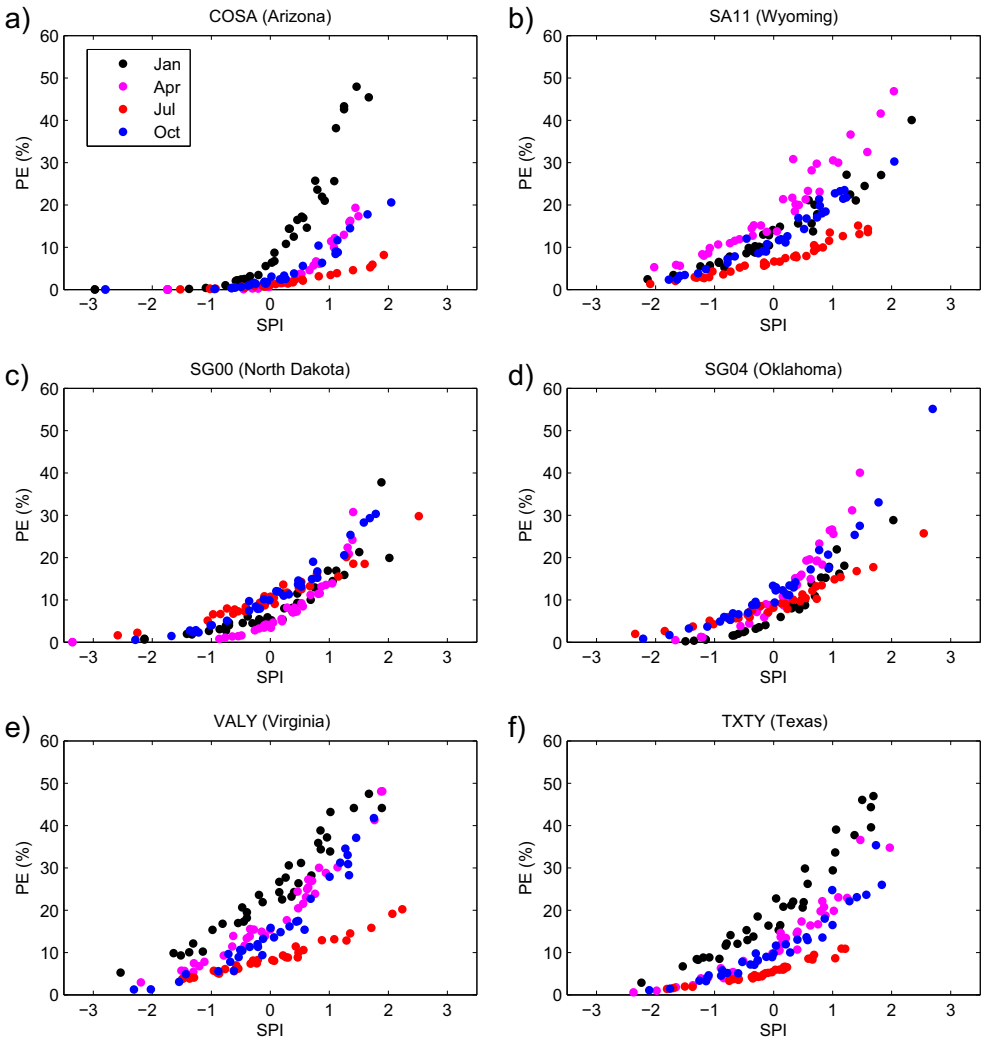

Fig. 9 PE versus SPI for selected months of the year. PE is computed using P from CPC data and PWV from ERAI reanalysis; the SPI is computed using P from CPC precipitation data. The common time period January 1979–April 2012 is considered. Units for PE are percent

SG00. In such cases, almost the same PE threshold is found for the different months of the year that varies only as a function of the SPI classes.

4 Conclusions

In this study, the potential of ground-based GPS measurements of atmospheric total column water vapor for monitoring meteorological wet/dry conditions outlined previously by Bordi et al. (2014b) is further explored. In particular, six GPS stations in the USA, which are part of the SuomiNet network, have been considered, and PWV data spanning from January 2007 to December 2012 have been analyzed on the timescale of interest (i.e., 1 month). The SPI time series on the 1-month timescale at grid points close to the stations are computed using gridded precipitation records from the NOAA CPC unified precipitation dataset available from January 1948 to April 2012. The availability of both PWV and P for a given location allows the computation of PE as a measure of the effectiveness of dynamic mechanisms in releasing the moisture in the air.

The comparison of GPS observations with PWV data taken from ERA-Interim reanalysis at grid points closest to the stations reveals satisfactory agreement, justifying the use of the ECMWF product for extending the analysis of PWV at the sites back to January 1979.

The overall results suggest that PWV time series are dominated by the seasonal cycle with maximum values during summer months, following the temperature annual cycle. Moreover, it is found that, for all stations and months of the year, PWV is only poorly correlated with actual recorded P and the SPI. However, PE highly correlates with the SPI, providing useful information on wet/dry spell occurrences. Long data records would allow, for each month of the year, the identification of PE thresholds associated with different SPI classes that have potential for forecasting wet spells. It is noted that for stations characterized by a seasonal behavior of PE, the threshold of PE for a given SPI class varies within the

year, a feature particularly evident for wet conditions (SPI greater than 1). Very low PE thresholds can be identified for dry conditions, but it is hard to distinguish variations for the different SPI dry classes (SPI less than −1).

Further efforts should focus on other regions characterized by different climate regimes, like the Mediterranean basin or subtropical areas. Of particular interest could be large river basins that require attention from a climatic and hydrological point of view. However, in any case for a given location, long data records of simultaneous measurements of PWV and P are necessary to carry out a comprehensive analysis. Given the estimate of PE thresholds for the different SPI classes based on climatological observations and forecasted PWV and P by numerical weather prediction models, it could be used to forecast future meteorological wet/dry events at a given location. Furthermore, the self-calibrating Palmer Drought Severity Index (scPDSI; Wells et al. 2004), which is widely used to monitor moisture conditions and takes into account not only precipitation but also temperature and evapotranspiration, could be considered in this kind of study. These will be topics of future investigations.

Acknowledgments PWV data from the SuomiNet GPS network have been freely retrieved from the website http://www.suominet.ucar.edu managed by the UCAR in Boulder, CO, USA. CPC US unified precipitation data are provided by the NOAA/OAR/ESRL PSD, Boulder, CO, USA, from their website at http://www.esrl.noaa.gov/psd/. ERA-Interim data have been provided by the ECMWF, Reading, UK, from their web site http://apps.ecmwf.int/datasets/. Support by the Max Planck Society is acknowledged (KF).

References

Beutler G, Brockman E, Frankhauser S, Gurtner W, Johnson J, Mervart L, Rothacher M, Schaer S, Springer T, Weber R (1996) Bernese GPS software 4.0, University of Berne

Bevis M, Businger S, Herring TA, Rocken C, Anthes RA, Ware RH (1992) GPS meteorology: remote sensing of atmospheric water vapor using the global positioning system. J Geophys Res 97: 15787–15801

Bevis M, Businger S, Chiswell S, Herring TA, Anthes RA, Rocken C, Ware RH (1994) GPS meteorology: mapping zenith wet delays onto precipitable water. J Appl Meteorol 33:379–386

Bevis M, Alsdorf D, Kendrick E, Fortes LP, Forsberg B, Smalley R Jr, Becker J (2005) Seasonal fluctuations in the mass of the Amazon River system and Earth's elastic response. Geophys Res Lett 32: L16308

Bock O, Guichard F, Janicot S, Lafore JP, Bouin M-N, Sultan B (2007) Multiscale analysis of precipitable water vapor over Africa from GPS data and ECMWF analyses. Geophys Res Lett 34:L09705. doi: 10.1029/2006GL028039

Bordi I, Sutera A (2004) Drought variability and its climatic implications. Glob Plan Chang 40:115–127

Bordi I, Fraedrich K, Sutera A, Zhu X (2014a) Ground-based GPS measurements: time behavior from half-hour to years. Theor Appl Climatol 115:615–625

Bordi I, Raziei T, Pereira LS, Sutera A (2014b) Ground-based GPS measurements of precipitable water vapor and their usefulness for hydrological applications. Water Resour Manag. doi:10.1007/s11269-014-0672-5

Borsa AA, Agnew DC, Cayan DR (2014) Ongoing drought-induced uplift in the western United States. Science. doi:10.1126/science.1260279

Brunner FK, Gu M (1991) An improved model for the dual frequency ionospheric correction of GPS observations. Manuscr Geodaet 16: 205–214

Davis JL, Herring TA, Shapiro II, Rogers AEE, Elgered G (1985) Geodesy by radio interferometry: effects of atmospheric modeling errors on estimates of baseline length. Radio Sci 20:1593–1607

Dee DP et al (2011) ERA-Interim reanalysis: configuration and performance of the data assimilation system. Q J R Meteorol Soc 137: 553–597

Duan J, Bevis M, Fang P, Bock Y, Chiswell S, Businger S, Rocken C, Solheim F, van Hove T, Ware R, McClusky S, Herring TA, King RW (1996) GPS meteorology: direct estimation of the absolute value of precipitable water. J Appl Meteorol 35:830–838

Gaffen DJ, Robock A, Elliot WP (1992) Annual cycles of tropospheric water vapor. J Geophys Res 97:18185–18193

Guerova G, Bettems J-M, Brockmann E, Matzler C (2004) Assimilation of the GPS-derived integrated water vapour (IWV) in the MeteoSwiss numerical weather prediction model — a first experiment. Phys Chem Earth 29:177–186

Guttman NB (1999) Accepting the Standardized Precipitation Index: a calculation algorithm. J Am Water Resour Assoc 35:311–322

Hagemann S, Bengtsson L, Gendt G (2003) On the determination of atmospheric water vapor from GPS measurements. J Geophys Res 108(D21):4678. doi:10.1029/2002JD003235

Hayes M, Svoboda M, Wall N, Widhalm M (2011) The Lincoln declaration on drought indices: universal meteorological drought index recommended. Bull Am Meteorol Soc 92:485–488

Higgins RW, Janowiak JE, Yao Y-P (1996) A gridded hourly precipitation data base for the United States (1963–1993). NCEP/Climate Prediction Center ATLAS No. 1. US Department of Commerce, Washington, 47 pp

Higgins RW, Shi W, Yarosh E, Joyce R (2000) Improved United States precipitation quality control system and analysis. NCEP/Climate Prediction Center ATLAS No. 7. US Department of Commerce, Washington

Houghton JT (1977) The physics of atmospheres. Cambridge University Press, Cambridge

Lutz JT (1977) Precipitation efficiency under varying atmospheric conditions. Geograph Bull 14:16–28

McKee TB, Doesken NJ, Kleist J (1993) The relationship of drought frequency and duration of time scales. Eighth conference on applied climatology, American Meteorological Society, Jan 17–23, 1993, Anaheim CA, pp. 179–186

Nakamura H, Koizumi K, Mannoji N (2004) Data assimilation of GPS precipitable water vapor into the JMA mesoscale numerical weather prediction model and its impact on rainfall forecasts. J Meteor Soc Jpn 82:441–452

Niell AE (1996) Global mapping functions for the atmosphere delay at radio wavelengths. J Geophys Res 101:3227–3246

Ortis de Galisteo JP, Bennouna Y, Toledano C, Cachorro V, Romero P, Andres MI, Torres B (2013) Analysis of the annual cycle of precipitable water vapor over Spain from 10-year homogenized series of GPS data. Q J R Meteorol Soc. doi:10.1002/qj.2146

Rocken C, Van Hove T, Ware R (1997) Near real-time GPS sensing of atmospheric water vapor. Geophys Res Lett 24:3221–3224

Saastamoinen J (1972) Atmospheric correction for the troposphere and stratosphere in radio ranging satellites. In: Henriksen SW, Mancini A, Chovitz BH (eds) The use of artificial satellites for geodesy. Geophys Monogr Ser, vol. 15, pp 247–251, AGU, Washington, D.C. doi:10.1029/GM015p0247

Seco A, González PJ, Ramírez F, García R, Prieto E, Yagüe C, Fernández J (2009) GPS monitoring of the tropical storm Delta along the Canary Islands track, November 28–29, 2005. Pure Appl Geophys 166:1519–1531

Smith TL, Benjamin SG, Gutman SI, Sahm SR (2007) Short-range forecast impact from assimilation of GPS-IPW observations into the Rapid Update Cycle. Mon Weather Rev 135:2914–2930

Sui C-H, Xiaofan L, Ming-Jen Y (2007) On the definition of precipitation efficiency. J Atmos Sci 64:4506–4513

Tuller SE (1971) The world distribution of annual precipitation efficiency. J Geogr 70:219–223

Ulich BL (1980) Improved correction for millimeter-wavelength atmospheric attenuation. Astrophys Lett 21:21–28

Vedel H, Huang X-Y, Haase J, Ge M, Calais E (2004) Impact of GPS zenith tropospheric delay data on precipitation forecasts in Mediterranean France and Spain. Geophys Res Lett 31:L02102. doi:10.1029/2003GL017715

Vey S, Dietrich R, Rülke A, Fritsche M (2010) Validation of precipitable water vapor within the NCEP/DOE reanalysis using global GPS observations from one decade. J Clim 23: 1675–1695

Ware RH, Fulker DW, Stein SA, Anderson DN, Avery SK, Clark RD, Droegemeier KK, Kuettner JP, Minster JB, Sorooshian S (2000) SuomiNet: a real-time national GPS network for atmospheric research and education. Bull Am Meteorol Soc 81: 677–694

Wells N, Goddard S, Hayes MJ (2004) A self-calibrating Palmer Drought Severity Index. J Clim 17:2335–2351

Xie P, Yatagai A, Chen M, Hayasaka T, Fukushima Y, Liu C, Yang S (2007) A gauge-based analysis of daily precipitation over East Asia. J Hydrometeorol 8:607–626

Zhang M, Lu B, Song W (1999) A method for dual-frequency ionospheric time-delay correcting using a C/A code GPS receiver. J Electron 16:66–72